Unraveling Reaction Pathways and Specifying Reaction Kinetics for Complex Systems

R. Vinu and Linda J. Broadbelt

Department of Chemical and Biological Engineering, Northwestern University, Evanston, Illinois 60208; email: v-ravikrishnan@northwestern.edu, broadbelt@northwestern.edu

Annu. Rev. Chem. Biomol. Eng. 2012. 3:29–54

First published online as a Review in Advance on January 13, 2012

The *Annual Review of Chemical and Biomolecular Engineering* is online at chembioeng.annualreviews.org

This article's doi:
10.1146/annurev-chembioeng-062011-081108

1947-5438/12/0715-0029$20.00

Keywords

pyrolysis, oxidation, rate coefficients, free radicals, Evans-Polanyi relationship, moment-based models, kinetic Monte Carlo

Abstract

Many natural and industrial processes involve a complex set of competing reactions that include several different species. Detailed kinetic modeling of such systems can shed light on the important pathways involved in various transformations and therefore can be used to optimize the process conditions for the desired product composition and properties. This review focuses on elucidating the various components involved in modeling the kinetics of pyrolysis and oxidation of polymers. The elementary free radical steps that constitute the chain reaction mechanism of gas-phase/nonpolar liquid-phase processes are outlined. Specification of the rate coefficients of the various reaction families, which is central to the theme of kinetics, is described. Construction of the reaction network on the basis of the types of end groups and reactive moieties in a polymer chain is discussed. Modeling frameworks based on the method of moments and kinetic Monte Carlo are evaluated using illustrations. Finally, the prospects and challenges in modeling biomass conversion are addressed.

INTRODUCTION

Mechanistic model: a detailed model developed using elementary reactions and their rate coefficients to describe the kinetics of a system

Reacting systems are often characterized by their complexity. Many natural and industrial processes, such as atmospheric ozone formation (1, 2); weathering of polymeric surfaces (3); combustion, partial oxidation, and cracking of hydrocarbons (4); incineration and pyrolysis of polymers and waste plastics (5); nanoparticle synthesis (6, 7); and biomass conversion (8), involve complex chemistry of hundreds of interacting species in thousands of reactions. Although the complications arising from these combinatorial reaction networks can be obviated by utilizing stoichiometric or yield-based lumped kinetic models, which result in simple analytical rate expressions that describe the overall macroscopic behavior of the system, these models do not quantitatively capture rates over wide ranges of operating conditions such as temperature, pressure, catalyst loading, or feed composition. This is because these models are strictly tailored for specific reaction conditions and feedstock properties, and their kinetics are not mechanistically based. Mechanistic or microkinetic models have the unique ability to determine which species or reaction pathway(s) is responsible for the observed system behavior, and hence provide a handle to optimize the process conditions for the desired outcome. Mechanistic models provide a quantitative understanding of the reaction system, as they unify experimental data, empirical correlations, and theoretical knowledge. Moreover, the potential to incorporate the rate coefficients of the various elementary steps determined through experiments, thermochemistry, surface science, statistical thermodynamics, structure-activity relationships, and quantum chemical calculations makes such models an appealing, albeit computationally expensive, prospect.

The most detailed mechanistic models to date have been developed for chemistries involving free radicals owing to the understanding of the reaction families and the availability of rate coefficients. Understanding of free radical reactions in the gas-phase and organic liquid-phase decomposition of long-chain organic molecules stems from the original work by Rice (9), who proposed a chain reaction mechanism more than 70 years ago and first demonstrated the formation of free radicals during the cracking of ethane. The elementary reaction steps include homolytic chain fission to form free radicals, cascades of hydrogen atom abstraction and β-scission steps to break down the molecule, and termination of the abundant radicals by coupling. Froment and coworkers (10, 11) first formalized automated generation of detailed kinetic models in terms of the above elementary steps using graph theory and Boolean relation matrices for the thermal cracking of paraffins, naphthalenes, olefins, and aromatics. This was followed by several efficient algorithms to implement kinetic models for related chemistries through the use of structure-oriented lumping (12), bond-electron matrices (13), rule-oriented programming (14), rank-based model reduction (15), and species and reaction elimination based on integer linear programming (16). Today, with the recent advancements in computer hardware (faster central processing units and graphics processing units), solution algorithms, and modeling tools such as Kinetic Model Editor (KME) (17), CHEMKIN (18), and DETCHEM (19), it is possible to visualize the course of reactions by coupling the kinetics with reactor transport equations. Some examples of classic mechanistic models developed to date for homogeneous systems include the oxidation of ethane (20), *n*-heptane (21), *iso*-octane (22), *iso*-cetane (23), and decalin (24); the pyrolysis of methane (25) and *n*-hexane (26); tropospheric ozone formation (1); and the atmospheric chemistry of volatile organic compounds and NO_x (2). A classic treatise on the foundation of molecular structure–based modeling and automatic reaction network generation for complex hydrocarbon feedstocks is available in Klein et al. (27). Excellent review articles by Poutsma (28, 29), Savage (30) and Ranzi et al. (4) discuss the various free radical reactions inherent in pyrolysis and oxidation as well as provide guidance on reasonable estimates of rate coefficients for the various elementary steps. Having provided a brief overview of the evolution of mechanistic models for homogeneous free

radical chemistry in general, we restrict our focus below to the kinetics of polymer pyrolysis and oxidation.

The mechanism of polymer decomposition by pyrolysis or oxidation is no different from the classic Rice-Herzfeld kinetics, and the basics of the modeling strategies available for hydrocarbon conversions are also applicable to polymeric systems. However, three key issues associated with polymeric systems make the modeling task more challenging. First, polymers are characterized by a distribution of chain lengths or molecular weights, which means that each and every polymer chain should be tracked during the reaction to obtain the properties of the polymer. This is one of the major hurdles to overcome in assembling the model, as it tremendously increases the number of species and reactions. Second, the possibility of branching and cross-linking reactions exacerbates the demand for bookkeeping to track the various branched species, networks, and their associated reactions. Importantly, the above two issues also seriously impact the execution time of the model solution. Third, because polymer decomposition involves a melt phase, the reptation, segmental, and translational diffusion of the two reacting chains governs the bimolecular termination rate, owing to the change in system viscosity with conversion (31). Hence, termination rate coefficients are not constant but instead vary with the chain length of the radicals and conversion, which requires the model to incorporate additional correlations. This review attempts to address the above issues in terms of their implementation in a mechanistic model.

BDE: bond dissociation energy

This article is organized as follows. We describe the various components of mechanistic models, e.g., reaction mechanism, specification of rate coefficients, construction of the reaction network, and choice of solution methodology, in the context of polymeric systems. Illustrative cases demonstrate the power of mechanistic models in unraveling reaction pathways. Finally, we close with the current scenario for modeling biomass fast pyrolysis and some suggestions for a path forward.

REACTION MECHANISM

Polymer Pyrolysis

The elementary steps involved in a Rice-Herzfeld chain mechanism can be broadly classified as radical-forming, radical-interconverting, and radical-consuming reactions. Radical-forming steps include homolytic cleavage of a polymer chain and molecular disproportionation. Radical-interconverting steps include hydrogen (H) abstraction, β-scission, and radical addition as well as intramolecular isomerization (backbiting) or H-shift reactions. Radical-consuming steps include termination of radicals by recombination or disproportionation. Detailed mechanistic models for the pyrolysis of vinyl polymers such as polystyrene (PS) (5, 32–35), polypropylene (PP) (36), and polyethylene (PE) (37–39) are well established. **Figure 1** depicts the various typical reaction families for pyrolysis of vinyl polymers.

Homolytic scission, which is the primary step in pyrolysis, is characterized by the random cleavage of a covalent bond along the main chain of a polymer. As shown in **Figure 1**, the main chain of vinyl polymers contains only one type of C–C bond. However, when the polymer has more than one type of C–C bond in the main chain (e.g., polybutadiene, polyisoprene), the bonds are preferentially broken on the basis of their bond dissociation energy (BDE). The BDEs of C–C bonds based on the character of C follow the order: vinyl C–vinyl C > vinyl C–allyl C > alkyl C–alkyl C > alkyl C–allyl C > allyl C–allyl C. Additionally, the BDE of a C–C bond depends on whether the C centers formed are primary (1°), secondary (2°) or tertiary (3°); 3° radicals are the most stable. Normally, in polymer pyrolysis models, the cleavage of C–H bonds is not considered because they are stronger than C–C bonds. A detailed listing of the BDEs of the various types of C–C and C–H bonds can be found elsewhere (29, 30). Molecular addition is the reverse of

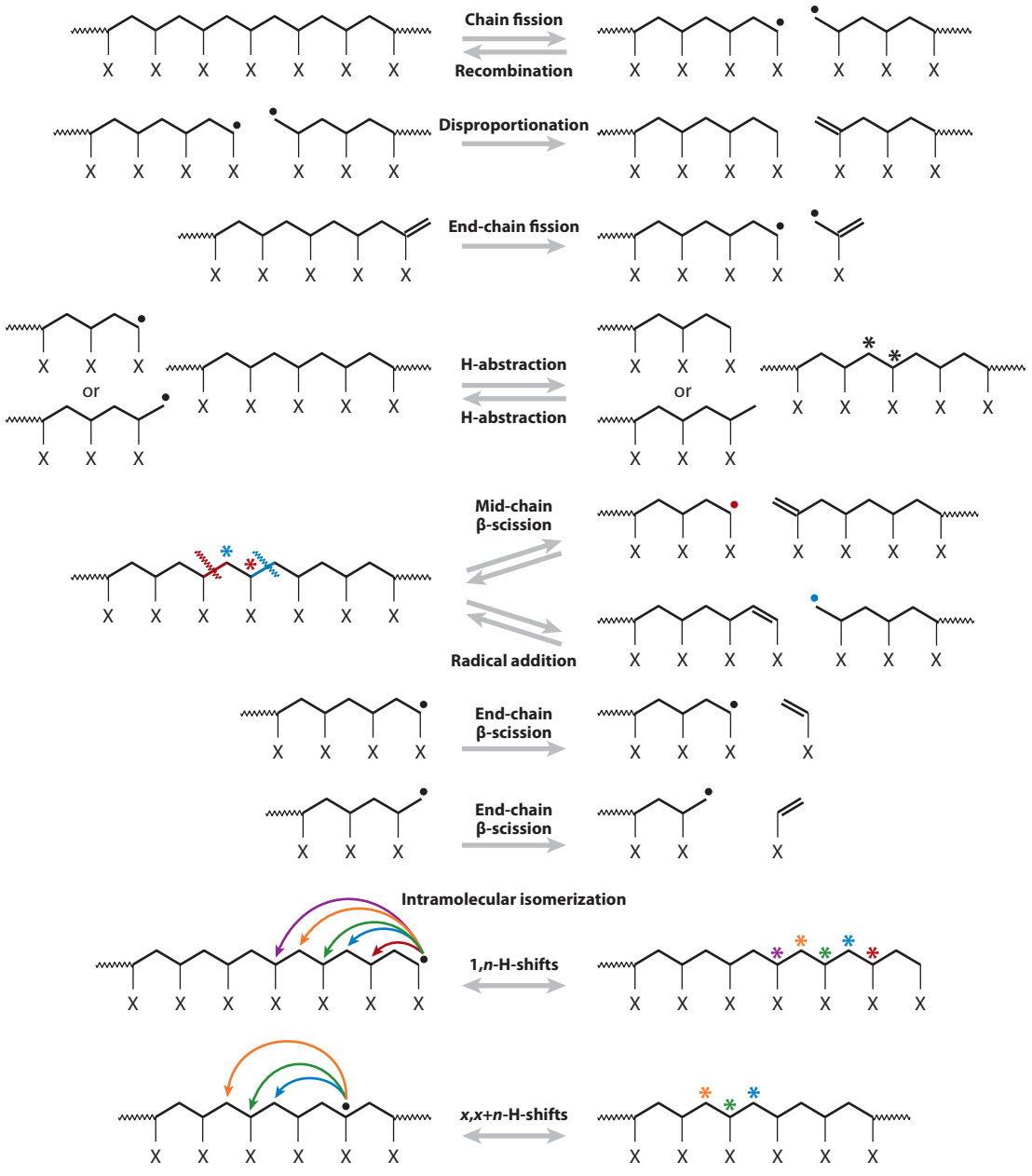

Figure 1

Various elementary reactions involved in the pyrolysis of vinyl polymers (5, 36, 37). X represents the substituent group; X = C_6H_5 for polystyrene, CH_3 for polypropylene, and H for polyethylene. The different possible radical sites are denoted by asterisks.

disproportionation, in which radicals form stable molecules. A detailed evaluation of this reaction shows that it is not competitive with homolytic fission under pyrolytic conditions (29). Rather, this reaction path is favorable only at low reaction temperatures, low concentrations of weak C–C bonds, and high concentrations of unsaturated species.

LMWP: low–molecular weight product

Reversible H-abstraction or chain transfer reaction to a polymer or low–molecular weight products (LMWPs) as well as β-scission are the major reactions that lead to the fragmentation of polymer chains. H-abstraction involves the cleavage of a C–H bond by hydrogen transfer to an abstracting radical. The abstracting radical and the product radical can be end-chain, mid-chain, or LMW radicals. Additionally, in polymer pyrolysis models, specific-mid-chain radicals are explicitly tracked to account for the formation of LMWPs by β-scission reactions. Owing to the many possible free radicals that can react with the polymers and LMWPs, H-abstraction is the major contributor to the complexity of polymer models in terms of the number of reactions. Unimolecular β-scission results in the cleavage of the bond in the β-position to the radical center, with the concomitant formation of a radical species and an unsaturated end. End-chain β-scission is a likely route to the formation of LMW radicals or LMWPs. Two extreme regimes are usually defined on the basis of whether end-chain β-scission or H-abstraction is the dominant reaction. In the moderate temperature and high substrate concentration limit, which is characteristic of liquid-phase polymerization, H-abstraction is dominant over end-chain β-scission, which is known as the Fabuss-Smith-Satterfield mechanism (29, 30). At the other extreme, where the temperatures are high and the concentration of the substrate is low, which is characteristic of pyrolysis, end-chain β-scission is dominant over bimolecular H-abstraction, and large amounts of LMW alkenes are formed. This is known as the Rice-Kossiakoff regime. Radical addition, which is one of the primary reactions in polymerization, is thermodynamically not favored at pyrolysis temperatures owing to the high negative value of the entropy, which overcomes the heat of reaction to increase the Gibbs free energy. However, it can be favored kinetically, as the addition of an end-chain radical to a π-bond competes effectively with the H-abstraction and end-chain β-scission reactions. The contribution of radical addition is significant during char formation in cracking reactions.

Another important reaction class that is essential for the formation of LMWPs and oligomers during pyrolysis is intramolecular isomerization. Also called H-shift reactions (such as 1,*x*-shift and *x*,*x*+*n*-shift), these reactions are primarily driven by how high the ring-strain energy of the cyclic transition state is. The ring strain for the various H-shifts follows the order (25) 1,3 (25.6 kcal mol^{-1}) > 1,4 (24.1 kcal mol^{-1}) > 1,5 (8.35 kcal mol^{-1}) > 1,6 (0.97 kcal mol^{-1}). These reactions compete with H-abstraction reactions that result in the formation of specific mid-chain radicals. Levine & Broadbelt (37) have shown using net rate analysis that during PE pyrolysis, a series of *x*,*x*+4-shifts were responsible for the formation of specific mid-chain radicals that undergo β-scission to form a range of C8–C24 alkanes and alkenes. Similarly, 1,7- and 7,3-shifts were found to be the major contributing reactions for the formation of 2,4-diphenyl-1-butene (styrene dimer) during PS pyrolysis (34). Estimates of the rate coefficients for the various 1,*x*-shifts are provided in **Supplemental Table 1** (follow the **Supplemental Material link** from the Annual Reviews home page at **http://www.annualreviews.org**).

Termination reactions can occur either by recombination of radicals (reverse of chain fission) or by disproportionation, which requires at least one radical to have a β-hydrogen. The exact mode of termination depends on the type of polymer, and various studies have shown that vinyl polymers terminate predominantly by recombination, whereas α-methyl vinyl polymers terminate by disproportionation (31). However, both forms of termination are always included in polymer models, and the ratio of the rate coefficients of recombination and disproportionation dictates their relative rates. Importantly, the recombination of an end-chain radical and a mid-chain radical can lead to the formation of a branched polymer species, which needs to be tracked during the course

of reaction. Once these branched species are formed, all other reactions apply for the branched species also. This creates a myriad of polymer species and reactions, and it is not practical to track each of them. One way to account for the reactions involving branches in the polymer chain is by lumping the branched species according to their end-group type, which is discussed below.

Arrhenius equation: rate coefficient, $k = A \exp(-E_a/RT)$, where A is the frequency factor and E_a is the activation energy

Polymer Oxidation

Detailed studies of oxidation of model hydrocarbon fuels and lubricant molecules have established a fundamental understanding of oxidation reactions (20–24, 40). The elementary steps in the oxidation of polymers, as taken from various studies (41–43), are depicted in **Supplemental Figure 1**. Oxidation chemistry clearly involves the formation of hydroxy, hydroperoxy, alkoxy, and alkylperoxy radicals, which take part in a series of β-scission, H-abstraction, hydroperoxide decomposition, and termination reactions to form species with aldehyde, ketone, alcohol, carboxylic acid, and ester groups. Although the mechanism is well known, a detailed mechanistic model for the oxidation of polymers is yet to be developed. This is partly because of the increased complexity of the model due to tracking the different groups that are generated during oxidation. We recently simulated the pyrolysis of poly(styrene peroxide) (PSP) as a model for the oxidation of PS (44). The major pyrolysis products of PSP, e.g., benzaldehyde and formaldehyde, are formed by β-scission of the alkoxy radical, and the minor products, α-hydroxy acetophenone and phenyl glycol, are formed by the successive H-abstraction of the LMW radicals and β-scission of the peroxy bond of the polymer chains. The model clearly shows that the presence or generation of even trace amounts of peroxy linkages in a polymer accelerates the degradation rate, owing to the low BDE of peroxy linkages compared with that of C–C bonds as well as the high rates of β-scission of the alkoxy radicals.

Although the above discussion indicates that the specification of an accurate mechanism is crucial for development of a successful polymer model, mechanism development is often an iterative process, and the mechanism may require revision until model outcomes match well with experiments. Moreover, given the many possible pathways for the formation of an experimentally observed product, a thorough understanding of the kinetics of the elementary steps is also required.

SPECIFICATION OF RATE COEFFICIENTS

Specification of reasonable values of the rate coefficients of the elementary steps in terms of the Arrhenius parameters, activation energy (E_a) and frequency factor (A) is vital for development of a mechanistic model. Many advanced analytical techniques such as laser flash photolysis, PLP-SEC (pulsed laser polymerization coupled with size exclusion chromatography), time-resolved fluorescence-absorption spectroscopy, electron spin resonance spectroscopy, and photon ionization mass spectrometry have enabled the generation, detection, and quantification of free radicals, and hence, the study of the kinetics of free radical reactions at a mechanistic level. PLP-SEC is a very useful technique to accurately determine propagation (k_p) and termination (k_t) rate coefficients in free radical homopolymerization and copolymerization. In particular, k_p values serve as reasonable estimates of the rate coefficient of the end-chain β-scission or depropagation reaction. After the extensive work of the International Union of Pure and Applied Chemistry (IUPAC) party for *Modeling of Polymerization Kinetics and Processes*, k_p and k_t values for a variety of alkyl methacrylates, alkyl acrylates, olefins, styrenes, and various other monomers are benchmarked (45). Reliable values of rate coefficients of many free radical reactions are available in the literature (46) and are archived in online databases (47, 48). Although experimentally determined rate coefficients are

available for many elementary reactions, they are not available for the majority of reactions that comprise mechanistic models of macromolecular systems. In such circumstances, thermochemical data, quantum chemical calculations, and structure-activity relationships commonly are used, often in conjunction, to estimate the rate coefficients.

Benson's group contribution method: a technique to estimate thermodynamic properties by summing the individual contributions of atom-centered groups to the property

GA: group additivity

Ab initio methods: first principles–based molecular orbital methods to solve the Schrödinger equation with a minimum number of approximations

Thermochemical Kinetics: Group Additivity

Thermochemical kinetics involves the use of transition state theory (TST) to estimate rate coefficients. TST assumes that the transformation of reactants to products proceeds through an activated complex (or transition state structure) that is in quasi-equilibrium with the reactants and converts to the products with a rate coefficient, defined by kinetic theory, equal to $k_B T/h$. The TST rate constant, k_{TST}, expressed in terms of thermochemical data, is given by (49)

$$k_{TST} = \frac{k_B T}{h}(c^o)^{\Delta\nu^\dagger} \exp\left(-\frac{\Delta G^{o\dagger}}{RT}\right) \quad 1.$$

where k_B denotes Boltzmann's constant, T is the temperature, h is Planck's constant, $\Delta G^{\circ\dagger}$ signifies the standard Gibbs free energy change between the reactants and the activated complex, $\Delta\nu^\dagger$ is the change in number of moles in going from the reactants to the transition state, and c° represents the standard state concentration, which is usually 1 atm (gas phase) or 1 M (liquid phase). The Arrhenius parameters can be evaluated by calculating k_{TST} as a function of T and regressing A and E_a from the standard Arrhenius plot.

Although the thermodynamic properties of the reactants can be evaluated using Benson's group contribution method (49, 50), the activated complex requires special consideration, as only specialized techniques such as femtosecond spectroscopy can be used to detect it experimentally. In a series of papers, Willems & Froment (51, 52) described a step-by-step procedure to estimate A and E_a of the elementary steps in hydrocarbon pyrolysis using an approach in which the geometries and resulting properties of activated complexes were estimated. The estimation of A requires the entropy of a parent molecule whose structure is similar to the activated complex as well as the entropy corrections owing to the translational, rotational, vibrational, and electronic degrees of freedom of the activated complex with respect to the parent molecule. E_a can be estimated by a structural contribution method, wherein E_a is calculated as a sum of the E_a of a reference reaction of the same reaction type and corrections owing to the structural differences between the reactants and products of the actual reaction with respect to the reference reaction. The rate coefficients estimated from thermochemical data using this approach were good approximations to measured values, and therefore they can be used as reliable initial guesses in a parameter-fitting process.

The accuracy of the rate coefficients evaluated using thermochemical data can be improved by coupling ab initio quantum chemical calculations with a group additivity (GA) procedure. Sumathi & Green (53) utilized ab initio methods to estimate the thermochemical properties of the activated complex and used this value to find the GA estimate of a supergroup, which characterizes the reactive moiety of the transition state. This method was rigorously tested for H-abstraction reactions from a wide variety of organic molecules and found to yield rate coefficients in good agreement with experimental data. Marin and coworkers (54–57) developed a GA method in which the transition state–specific groups are modeled at three levels, e.g., primary or reactive group, which occurs at the line of making or breaking of the bond; secondary group with next-nearest neighbor interactions; and tertiary group to account for non-nearest-neighbor interactions. Thus, the sum of GA values of all the transition state–specific groups can be used to evaluate the relative change in state functions of the activated complex with respect to the reactants ($\Delta H^{\circ\dagger}$ and $\Delta S^{\circ\dagger}$) and hence, E_a and A. Saeys et al. (54, 55) and Sabbe et al. (56, 57) utilized this approach to

find the rate coefficients of β-scission, radical addition, and H-abstraction reactions of a range of hydrocarbon molecules and radicals; the rate coefficients found by GA were in good agreement with ab initio calculations.

PES: potential energy surface

DFT: density functional theory

Evans-Polanyi (E-P) relationship: $E_a = E_o + \alpha\Delta H_{rxn}$, where E_o is the E_a of a reference reaction of the same family, and α is the transfer coefficient

Quantum Chemistry Methods

The previous section introduced ab initio quantum chemical calculations and their role in improving the accuracy of GA methods, and hence, the speed of rate coefficient evaluation. However, quantum chemistry methods can be used to probe the kinetics of individual elementary steps without the concomitant development of a GA scheme. Computational quantum chemistry involves solving the electronic Schrödinger equation at various levels of approximations to determine the potential energy surface (PES), which corresponds to the energy of the reactant(s) as a function of its geometry. Ab initio methods are first principles–based approaches that use a minimal number of approximations to determine the PES; density functional theory (DFT) approaches are based on first principles but utilize electron density rather than the wave function to obtain the PES. The importance of quantum chemical computations in unveiling the reaction mechanisms and kinetics of complex reactions are described by Broadbelt & Pfaendtner (58) and Coote (59). With the power of computational hardware and the efficient algorithms implemented in computational suites, quantum chemical modeling is becoming more widely practiced to unravel reaction mechanisms and pathways for a wide array of macromolecular reactions.

Quantum calculations are useful in studying the variation of k_p values with chain length during the early stages of monomer addition during free radical polymerization, especially when the chain length dependency of k_p is difficult to determine experimentally (60, 61). Many studies have also demonstrated the use of quantum chemical calculations to accurately predict k_p values and monomer and radical reactivity ratios during copolymerization of vinyl monomers including methacrylates, acrylates, styrene, and vinyl acetate (62–64). Van Cauter et al. (65) addressed defect formation in poly(vinyl chloride) (PVC) during free radical polymerization by studying head-to-head versus head-to-tail addition using DFT methods. On the basis of the k_p values of the various monomer additions, head-to-head addition occurs at a rate of 2 per 1,000 vinyl chloride additions. Recently, Coote and coworkers (43) studied the propagation step in polymer autoxidation, wherein H-abstraction by the peroxy radical forms the polymer radicals. Their results indicate that, for a majority of regular polymers, this step is characterized by a large positive Gibbs free energy (10–65 kJ mol^{-1}) and is thermodynamically favorable only when the product radical is stabilized by an adjacent double bond or the presence of structural defects such as internal double bonds. These examples illustrate that quantum chemical calculations yield valuable information that serves as direct inputs to polymer mechanistic models and greatly improves their predictive power.

Structure-Activity Relationships

It is tedious or computationally infeasible to evaluate the rate coefficients for every reaction in many complex systems of $O(10^3 - 10^5)$ reactions using either of the above two approaches. Hence, it is efficient to use both experimental data and theoretical computations to devise correlations between E_a and thermodynamic properties based on the structure of the reacting species and the reaction family. One of the classic relations that is widely used in pyrolysis and oxidation mechanisms is the Evans-Polanyi (E-P) relationship (66), which states that the difference in E_a between two reactions of the same family is proportional to the difference in their heats of reaction. Stated in a simple form, $E_a = E_o + \alpha\Delta H_{rxn}$, where E_o is the activation energy of the reference reaction of the same class, and α characterizes the position of the transition state along the reaction

coordinate such that $0 \leq \alpha \leq 1$, and $\alpha_{\text{forward rxn.}} = 1 - \alpha_{\text{reverse rxn}}$. The E-P relationship assumes that the frequency factor and the position of the transition state along the reaction coordinate are the same for all reactions belonging to a particular reaction family. A compiled set of E-P parameters and a reasonable range of A values from different sources for the various elementary steps involved in pyrolysis and oxidation are provided in **Supplemental Table 1** (41, 67–75). The value of α need not always be positive or bound between zero and one, as was shown in a recent study of H-abstraction by alkylperoxy radicals in which hydrogen-bonded precomplexes (ROOH···R′), whose binding energy increases with reaction exothermicity, can result in negative α values when properties of the unbound reactants and products are used in the correlation (75).

Structure-activity correlations are not always linear, as electron transfer, atom transfer, and certain radical addition reactions exhibit nonlinear trends in E_a versus ΔH_{rxn}. One of the well-known relationships for electron transfer reactions is the Marcus equation (76), which predicts an inverted behavior of E_a for highly exothermic reactions. However, for atom transfer reactions (e.g., H-abstraction), Blowers & Masel (76) developed the following modified form of the Marcus equation to predict the trend of $E_a \to 0$ for extremely exothermic reactions, $E_a \to \Delta H_{rxn}$ for highly endothermic reactions, and Marcus behavior in between:

$$E_a = \begin{array}{cc} 0 & \Delta H_{rxn}/4E_o < -1 \\ E_o\left(1 + \Delta H_{rxn}/4E_o\right)^2 & -1 \leq \Delta H_{rxn}/4E_o \leq 1 \\ \Delta H_{rxn} & \Delta H_{rxn}/4E_o > 1 \end{array}. \qquad 2.$$

By investigating carbon-centered radical addition to alkenes, Fisher & Radom (77) have shown that E_a is determined not only by the reaction enthalpy but also by polar charge transfer as well as the electrophilicity and nucleophilicity of the polar substituents. This has led to a nonlinear E-P-like equation, given by $E_a = (E_o + \alpha\Delta H_{rxn})F_eF_n$, where F_e and F_n are electrophilic and nucleophilic factors, respectively. This relationship satisfactorily describes the trends in E_a for the addition of a wide variety of radicals (such as alkyl, allyl, diallyl, benzyl, vinyl, phenyl, and propargyl) to alkenes (56). Another technique that has attracted interest for its potential in unraveling the mechanisms of and rate coefficients for thermal decomposition of polymers is reactive molecular dynamics, which is described in the sidebar (78–81). In modeling complex systems, for which one mostly utilizes rate coefficients evaluated by any of the above techniques from diverse sources, care must be exercised to ensure that thermodynamic consistency is met, i.e., the equilibrium constant, $K_a = \exp(-\Delta G^o_{rxn}/RT)$ (49).

REACTIVE MOLECULAR DYNAMICS

Reactive molecular dynamics (RMD) is a simulation technique that is used to dynamically explore reaction pathways at an atomistic level without a priori knowledge of the kinetics. RMD integrates classical molecular dynamics with reactive force fields to describe the transformations of the covalent bonds during reaction, and hence the PES. Smooth transition from reactants to products along the reaction coordinate is facilitated by switching functions, which describe the bond energy-bond order relationships (78). RMD allows the force-field parameters of the model compounds, e.g., BDEs and bond lengths, to be determined independently using high-level ab initio and coupled cluster quantum calculations, thus enabling an estimation of the kinetic parameters of the elementary steps. RMD is currently being employed to study the condensed-phase high-temperature decomposition of high–energy density materials such as RDX (cyclotrimethylene trinitramine) (79) as well as thermal degradation of polymers such as PE (78), PP (78), poly(methyl methacrylate) (80), and poly(isobutylene) (81).

Table 1 Various functional forms used to describe chain length dependency of $k_t^{i,j}$ (31)

Functional form	$f(i,j)$	Rate-determining step
Harmonic mean	$\left(\frac{2ij}{i+j}\right)^{-\alpha}$	Chain-end encounter or coil overlap
Smoluchowski mean	$0.5(i^{-\alpha}+j^{-\alpha})$	Translational diffusion
Geometric mean	$(ij)^{-\alpha/2}$	Segmental diffusion

Accounting for Chain Length Dependencies

This section evaluates the origin of the chain length dependency exhibited by termination rate coefficients and appropriate ways to implement them in a mechanistic model. The rate of termination of propagating radicals by combination or disproportionation is controlled by the translational, or center of mass, diffusion of the highly mobile radical chains at low conversions of the monomer, segmental diffusion or reptation of the relatively immobile radical chains in the medium- to high-conversion range, and reaction diffusion of the monomeric radicals to terminate the immobile radical chains at the high-conversion limit. Usually, k_t for the termination of radicals of length i and j is expressed as, $k_t^{i,j} = k_t^{1,1} f(i,j)$ (31), where, $k_t^{1,1}$ is the termination rate coefficient for radicals of chain length 1. The functional form of $f(i,j)$ is based on the type of diffusion and conversion regime as shown in **Table 1**. The exponent, α, signifying the chain length dependency, can be determined by PLP, and values of α are available for a range of monomers. Smoluchowski's mean is the preferred description of chain length dependence of k_t, as it is consistent with the Rouse model for polymer chains within the entanglement limit when $\alpha = 1$ (82) and also consistent with the reptation model for chains above the entanglement limit when $\alpha = 2$ (83). Keramopoulos & Kiparissides (84) have modeled the diffusion-controlled propagation and termination rates during free radical polymerization using Smoluchowski's diffusion equation, which is given by

$$\frac{1}{k_p} = \frac{1}{k_{p,0}} + \frac{1}{4\pi r_t D_m N_A}; \quad \frac{1}{k_t^{i,j}} = \frac{1}{k_{t,0}^{i,j}} + \frac{1}{4\pi r_t D_p N_A}, \qquad 3.$$

where $k_{p,0}$ and $k_{t,0}^{i,j}$ denote the intrinsic propagation and termination rate coefficients; r_t denotes the effective reaction radius; D_m and D_p signify the diffusion coefficients of the monomer and polymer chains, respectively, which are calculated using free-volume theory; and N_A denotes Avogadro's number. Although this approach requires the specification of the physical and transport properties of the reacting system, the different diffusion regimes are inherent in the above expressions, and hence, there is no requirement to explicitly specify the rates at different limiting conditions. Although the above discussion treats recombination ($k_{t,c}$) and disproportionation ($k_{t,d}$) as a single termination rate coefficient, both modes of termination exhibit diffusion dependencies, and their actual values differ on the basis of the structure of the radicals. Rate coefficients of self- and cross-radical combination ($k_{t,c}^{1,1}$) and disproportionation ($k_{t,d}^{1,1}$) of a variety of alkyl-, allyl-, vinyl-, and phenyl-substituted alkyl radicals have been experimentally determined (68–71, 85), and the ratio $k_{t,c}^{1,1}/k_{t,d}^{1,1}$ can be used to specify $k_{t,c}$ and $k_{t,d}$.

Polydispersity index (PDI): measure of the breadth of the molecular weight distribution of a polymer; PDI = M_w/M_n

KMC: kinetic Monte Carlo

CONSTRUCTION OF THE REACTION NETWORK

The next step in the model development process is to define the methodology by which the stable polymeric species, polymeric radicals, LMWPs, and LMW radicals are tracked during the reaction. Ideally, the complete topology of each and every long-chain molecule needs to be tracked to monitor the exact distribution of the chains. This is not an impossible task, but it is limited by the chain length, polydispersity index (PDI), and number of elementary steps in the reaction system. By using probabilistic models based on kinetic Monte Carlo (KMC), each

and every species can be tracked during polymerization or degradation. Wang & Broadbelt (86, 87) have developed a KMC model to track the explicit sequences that are generated in gradient copolymers of styrene and methyl methacrylate (MMA) during nitroxide-mediated controlled radical polymerization (NM-CRP). Copolymers of chain length up to 2,000 and PDI of 1.68 were simulated. However, unlike polymerization, pyrolysis and oxidation of polymers result in the formation of many different functional groups, and tracking each and every chain can become expensive. Our recent KMC model for PSP pyrolysis involved 949 specific reactions of 83 species without any branching reactions (44). The simulation was, however, performed with an initial chain length of 20 and unit PDI. Longer chain lengths dramatically increased the simulation time.

MWD: molecular weight distribution

It is, hence, imperative that continuum models with lumping of species at some level be developed to study the pyrolysis and oxidation of high–molecular weight polymers (chain length $\geq$ 1,000). A class of models has lumped the entire polymer and radical species into polymer and radical groups, respectively (88–90). Although these lumped models, which lack any structural details of the polymer or radicals, yield analytical rate expressions that are useful to determine the time evolution of polymer concentration and molecular weight distribution (MWD), the mechanistic details are hidden, and hence, these models lack predictive power. Moreover, the rate coefficients in these models, which are usually determined by fitting against the experimental data, signify the overall degradation rate and not that of any elementary step(s) involved in the reaction. One of the simplest ways to account for the structural details of the polymers is to track the end groups characterizing the polymer chains. **Figure 2** depicts the end groups that were utilized to track the various long-chain polymers and radicals during the pyrolysis of vinyl polymers. The scaling of polymer pyrolysis model complexity, in terms of the number of species and reactions, with respect to the number of end-group and radical types, is given in **Table 2** (36, 37,

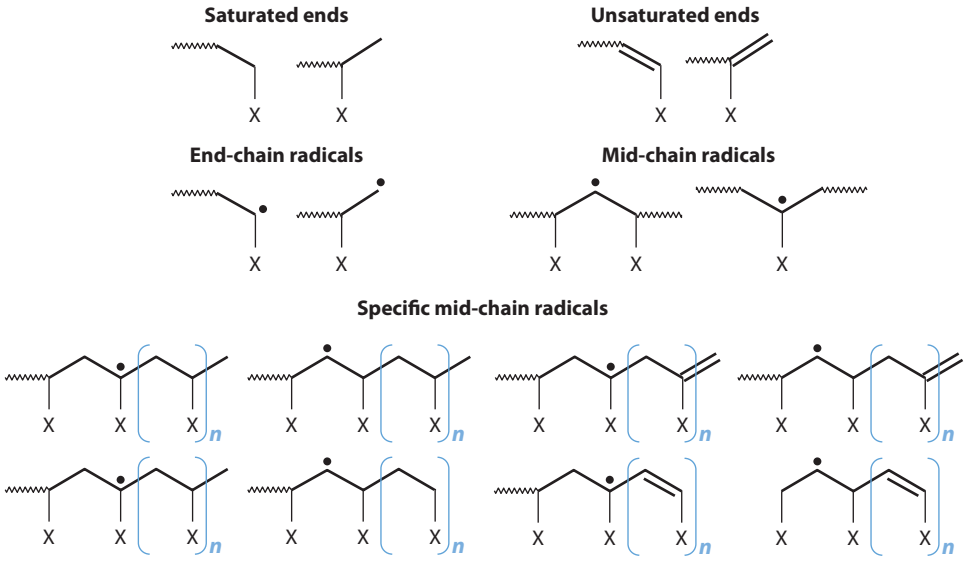

Figure 2

Various end-chain and mid-chain types used in mechanistic models for the degradation of vinyl polymers (5, 36, 37). X represents the substituent group; X = C_6H_5 for polystyrene, CH_3 for polypropylene, and H for polyethylene. The number of end-chain types is greatly reduced when X = H.

Table 2 Scaling of complexity of polymer pyrolysis models with the number of polymer and radical types

Polymer	Species	Reactions	Polymer end types	End-radical types	Mid-radical types	Specific mid-radical types	Reference
PS	93	4,502	4	2	2	5	92
PP	213	24,480	4	2	2	21	36
PE	151	11,007	2	1	1	24	37
PS/PP	277	37,409	8	4	4	25	91
Polyisoprene	440	$>10^5$	6	6	2	18	R. Vinu & L.J. Broadbelt, unpublished data

Abbreviations: PS, polystyrene; PP, polypropylene; PE, polyethylene.

91, 92; R. Vinu & L.J. Broadbelt, unpublished data). The number of species and reactions clearly increases with both the number of end-group types and the specific mid-chain radicals that are tracked during the reaction. Furthermore, in the case of pyrolysis of a mixture of polymers, the number of reactions increases further owing to the interactions between the two polymers. The level of interaction depends on the miscibility of the two polymer melt phases. Kruse et al. (91) handled these interactions by incorporating cross H-abstraction reactions and allowing a fraction of LMW radicals derived from PS to react with PP, and vice versa, to capture the enhancement in the pyrolysis rates of PP in the presence of PS.

Characterization of the polymers by their end-group types is necessary but not sufficient. During recombination and radical addition steps, formation of atypical bonds, i.e., head-to-head and tail-to-tail linkages, is possible in the polymer chain. These structural irregularities in the polymer may create weak links that possess high rates of bond cleavage. Hence, the formation and disappearance of these links needs to be tracked explicitly by utilizing rate equations for the different types of bonds and incorporating probabilities in the rate expression to account for the relative population of the bonds. As mentioned above, branched polymeric species and radicals also participate in the elementary steps, and it is important to devise strategies to track them explicitly during the reaction. Kruse et al. (5) have adopted a lumping approach to group the branched species on the basis of three criteria: the chain end type of the branch fragment (saturated/unsaturated), average number of branches (N_{br}), and the fraction of branched species with one branch. The value of N_{br} was determined from the number of chain end types that exist in a branched species (N_{end}), according to the expression $N_{br} = N_{end} - 2$. The fraction of chains with more than one branch was assumed to decrease according to the geometric distribution. The probability of a branched polymer chain with an additional branch can be evaluated as $P = 1 - N_{br}^{-1}$. **Figure 3** depicts the four different types of branch point and non-branch point β-scission reactions along with their scission probabilities. Polymer pyrolysis models developed by Ranzi and colleagues (38) also track the radicals at the branch and non-branch points in a polymer chain. Finally, characterization of the char and condensed fragments during pyrolysis is another important issue in polymer pyrolysis models, as specific structures cannot be assigned to these carbonaceous species. Marongiu et al. (93) have utilized pseudocomponents to represent the condensed species and radicals at different levels of cross-linking in terms of the number of benzene rings in the structure during PVC pyrolysis. Their semidetailed model satisfactorily captured the experimental trends.

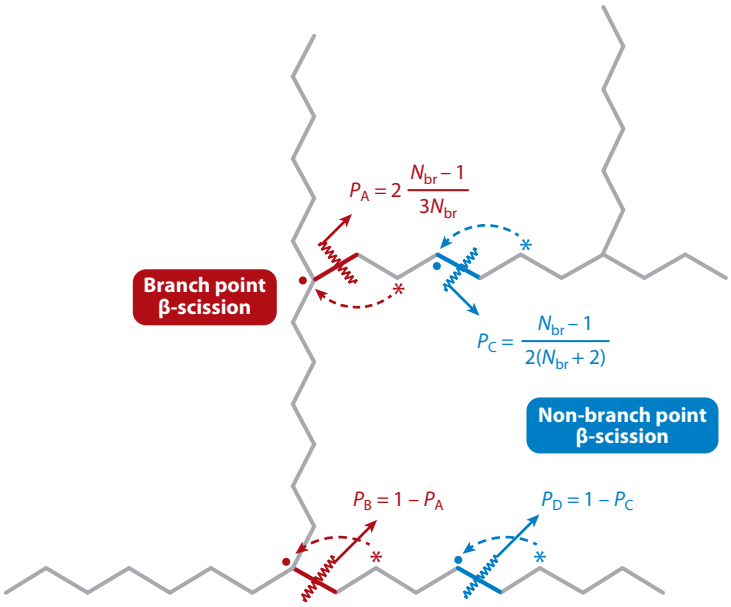

Figure 3

Two different possibilities for branch point and non-branch point β-scission in branched polymers (5). The formation probabilities of two branched species as well as a branched and a linear species are shown. Dashed arrows indicate that a mid-chain radical (denoted by an asterisk) is transformed to an end-chain radical (denoted by a solid dot) after β-scission.

MODELING FRAMEWORK

Moment-Based Models

Having specified the mechanism, rate coefficients, and species identity in terms of the end groups and lumping rules, it is important to develop rate equations and any accompanying approximations to solve the model as well as evaluate the time evolution of polymer concentration and MWD. As polymer molecules and radicals are characterized by a distribution of chain lengths, continuum models usually treat polymer concentration as a function of both chain length, x, and time, t, as $p(x,t)$. The resulting integro-differential rate equations can be solved either by transforming them to ordinary differential equations by the application of moments or by carrying out a full numerical simulation. The former method is more relevant to and widely practiced for mechanistic models owing to the complexity involved. Various modes of polymer chain scission, e.g., random chain fission, chain end fission/β-scission, and preferential midpoint fission, are characterized by stoichiometric kernels, $\Omega(x,x')$, that describe the chain length distribution when a polymer of chain length x' undergoes scission to form polymers (or radicals) of chain length x and $x' - x$ (94, 95). The most widely used kernels correspond to $1/x'$ for random fission, $\delta(x' - x_s)$ for end-chain fission/β-scission, and $\delta(x - x'/2)$ for mid-chain fission. Moreover, the random fission rate coefficient was found to depend on the chain length and position of the bond along the chain. Many studies have assumed a fission rate coefficient of the form $k_f(x) = k_f\, x^\lambda$ and evaluated the stability and scalability of the solutions with λ and the recombination reaction (96–98). When $\lambda < -1$, the system becomes unstable owing to spontaneous and cascading breakup to monomers, and $\lambda = 1$ satisfactorily describes random fission (96). Similarly, H-abstraction rate coefficients are also assumed to be

Moment: the nth moment of $p(x,t)$ is defined as $p^{(n)}(t) = \int_0^x x^n p(x,t)\mathrm{d}x$

linearly dependent on the chain length of the polymer, as the availability of abstractable hydrogen atoms increases with chain length. Usually, the assumption of the linear dependence of fission and H-abstraction rate coefficients on chain length leads to what is known as the closure problem, i.e., the rate equations for lower-order moments are dependent on higher-order moments. Based on the nature of the MWD, different approximations exist for the third moment in terms of the lower moments. A well-known approximation based on a gamma distribution that is well suited for $1.5 < \text{PDI} < 2$ is that of Saidel & Katz (99), which is given by $p^{(3)} = 2p^{(2)^2}/p^{(1)} - p^{(2)}p^{(1)}/p^{(0)}$.

Teymour and coworkers (100) have developed a weighted sum approximation based on both gamma and log-normal distributions to characterize gelation ($\text{PDI} \gg 2$), which is caused by cross-linking and extensive branching. An expression for the third moment can also be derived using the skewness of a distribution from first principles (101). The moment equations for the various elementary steps in polymer pyrolysis and polymerization are described elsewhere (5, 102). The moment solutions correspond to the molar concentration (zeroth moment), mass concentration (first moment) and variance (second moment) of the polymer MWD. The number average molecular weight (M_n), weight average molecular weight (M_w), and PDI of the polymer can be calculated as $p^{(1)}/p^{(0)}$, $p^{(2)}/p^{(1)}$, and M_w/M_n, respectively.

Long-chain approximation (LCA): reactant disappearance is primarily due to propagation reactions under the long kinetic chain limit, whereas initiation and termination reactions affect only overall reaction progress

Pseudo–steady state approximation (PSSA): the rate of formation of short-lived radical species can be equated to the rate of their disappearance

The solution of and kinetic analysis of complex reaction networks can be simplified by utilizing the long-chain approximation (LCA) and the pseudo–steady state approximation (PSSA). LCA asserts that the reactant disappears primarily owing to the propagation reactions under the long kinetic chain limit, and PSSA states that the net rate of formation of the radical species can be equated to zero (103, 104). Although the application of PSSA greatly reduces the dimension of the system of equations by providing analytical solutions to radical concentrations, its application is limited to mechanisms involving only a few steps, as it is laborious to derive such expressions for large mechanisms.

The shape and width of the MWD control the structural, mechanical, optical, and rheological properties of the polymer, and hence, it is critical to determine the MWD of the polymer during degradation or polymerization. There are many methods to calculate the polymer MWD. A numerical method involves solving the population balance rate equations explicitly by utilizing various discretization algorithms such as the sectional grid method, orthogonal collocation, and the Galerkin method (105). Probability-generating function (pgf) transformations can also be used to predict the full MWD by transforming the polymer and radical balance equations according to the pgf to solve the finite set of differential-algebraic equations and then numerically inverting the result (106). Within the method of moments framework, the form of the polymer MWD is assumed, and the distribution is expressed in terms of the polymer and radical moments. Kruse et al. (107) have utilized Schultz (gamma) and Wesslau (log normal) distributions to predict the MWD during the pyrolysis of PS. As the initial polymer and the polymer chains formed by β-scission reactions were explicitly tracked in the mechanistic model, a Schultz distribution satisfactorily captured the evolution of a bimodal distribution during degradation. However, during gelation and post-gel formation, the higher-order moments diverge to infinity, and the moment approach alone cannot be used to model the MWD. To address this issue, the numerical fractionation approach was developed (108, 109), which allows the moments to be applied to the various generations of the soluble (sol) fraction on the basis of the structure of the polymer and the size of branches. The overall MWD can be obtained by summing the distributions of the individual generations.

The next step in the modeling process is to develop methods by which the entire reaction network and the rate equations can be generated on the fly. This requires a parsing grammar to be implemented according to the elementary reaction rules in a scripting language. Although commercial mechanism-generation packages are available for studying pyrolysis and oxidation of hydrocarbon molecules [e.g., KME (17), XMG (25), SPYRO (110)], none is available for polymeric

systems. This is partly because universal rule-based generation of reactions is rendered difficult owing to the diversity in the structure of different classes of polymers and the different pathways that each polymer takes during degradation. Broadbelt and colleagues (5, 34, 36, 37) have developed programs that, given the chain end and radical types, automatically generate the species, reactions, moment equations, and algebraic equations for both polymerization and degradation of vinyl polymers. The stiff set of differential-algebraic equations can then be integrated with numerical solvers [such as DDASAC (111) or LSODE (112)] and parameter optimization routines [such as GREG (113)] to simulate the kinetics. We are currently extending it to model the degradation of natural and synthetic elastomers. For polymerization systems, PREDICI®, which is based on the Galerkin h-p method, is commonly used for process modeling, determination of MWD, and rate coefficient estimation (114).

One of the primary advantages of mechanistic models lies in the analysis of the relative importance of the different pathways using sensitivity analysis and net rate analysis. Sensitivity, S_{ij}, of the concentration of species i, C_i, to the reaction j, k_j, given by $S_{ij} = \frac{\mathrm{d}\ln C_i}{\mathrm{d}\ln k_j}$, is a useful measure of the dominant reaction channel taken by a particular species. Complementarily, the net rate or the sum of the rate contributions of all the species through a specific elementary step determined from the rate equations can be used as a valuable tool to unravel the pathway(s) of formation of the various products. The evolution of styrene, 2,4-diphenyl-1-butene (dimer), and 2,4,6-triphenyl-1-hexene (trimer) during the pyrolysis of PS is a classic example of a system whose mechanism is still questioned, albeit well studied. Although it is well accepted that styrene is formed by end-chain β-scission and the trimer is formed by 1,5-shift followed by β-scission, the mechanism of dimer formation has long been unaddressed. A conventional route to the dimer involves 1,3-shift followed by β-scission, but this is not kinetically favorable owing to the high ring strain energy of the 1,3-intramolecular H-shift. Levine & Broadbelt (34), based on the ab initio calculations of high-temperature styrene polymerization by Moscatelli et al. (115), incorporated 1,7-shift, followed by 7,3-shift and β-scission, to model dimer evolution. Besides prediction of the experimental time evolution of the products, the model also provides mechanistic insights. The competing pathways for the formation of the dimer are depicted in **Figure 4**. Net rate analysis showed that the 7,3-shift competes with the benzyl radical addition pathway to form the secondary benzyl radical at the third position, which serves as a precursor of the dimer. The 7,3-shift was ten times more dominant than the benzyl radical addition at low temperatures (~310°C), whereas at higher temperatures

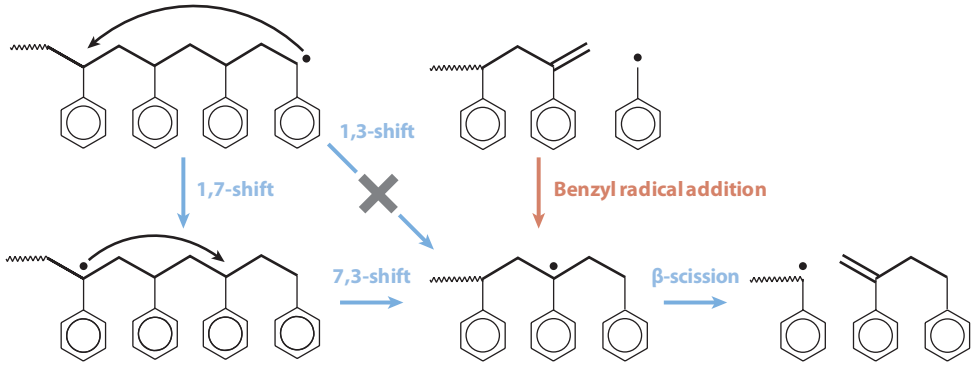

Figure 4

Reaction pathways for the formation of styrene dimer during the pyrolysis of polystyrene (*blue arrows*) (34). The competing benzyl radical addition pathway is shown with a brown arrow.

(>350°C), the contribution of benzyl radical addition was significant. Recently, another study has suggested that the inclusion of a small or finite amount of 1,7-shift could actually improve the model prediction of the tetramers during PS pyrolysis (35).

Stochastic simulation algorithm (SSA): a Monte Carlo procedure to numerically generate the temporal evolution of species populations

Kinetic Monte Carlo Methods

KMC, a probabilistic simulation technique, is an alternative to continuum models to study the kinetics of chemically reacting systems. KMC has its foundation in the stochastic chemical master equation, which determines the probability that a species would have reacted and that it has a specific molecular population at a future time. Gillespie (116, 117) has formulated a stochastic simulation algorithm (SSA) to compute the time evolution of the species population in exact accordance with the master equation (see **Supplemental Table 2**). One of the primary motives for using KMC to model polymer systems is that the traditional moment-based models require numerical solvers to solve stiff sets of coupled differential-algebraic equations, whereas KMC models utilize an iterative approach, and hence, difficulties such as the stiffness of the system are not encountered.

KMC models track discrete particles in a scaled homogeneous reaction volume instead of overall species concentrations. This means that explicit polymer chain sequences can be tracked, unlike the lumped polymer chains based on the end groups that are tracked in moment-based models. This attribute of KMC models makes them ideal to study MWDs in branched and cross-linked polymers, which otherwise are difficult to study using moment-based models. In a series of papers, Tobita (118–120) derived analytical expressions to describe the time evolution of MWD, average molecular weight, and gel point during the degradation of star-shaped and multibranched polymers using random sampling and chain scission probabilities. The PDI of a star polymer with f arms was found to evolve to a limiting value of $(1 + f)/f$. In another detailed study of degradation of linear polymers, Bose & Git (121) utilized a stochastic binary tree scission model to describe the temporal evolution of MWD during mid-chain, percent-cut, and unzipping scissions. Although these studies demonstrated the value of Monte Carlo for understanding the property changes of a polymer during branching and chain scission, they do not incorporate any mechanistic and kinetic details specific to a polymer system.

One pathway-level model using KMC is McDermott et al.'s (122) study of the degradation of poly(veratryl β-guaiacyl ether), a model lignin compound. Their KMC approach was based on fixed time steps and is outlined in **Supplemental Table 2**. Polymers were considered to behave like Markov chains, which react according to the transition probabilities of the reaction type. This approach allows more than one reactive site to be considered at a given time interval for reaction. This approach was also validated for the acid hydrolysis of cellobiose and amylose (123). We have utilized Gillespie's SSA to model the pyrolysis of PSP (44) and shown that H-abstraction plays an important role in the generation of LMW alkoxy radials, which serve as precursors for the formation of minor products, namely, α-hydroxyacetophenone and phenyl glycol. **Supplemental Figure 2** shows that the model prediction of peroxide concentration profiles and final product yields compare well with experimental data. The KMC model tracked a range of dimers that differed by head/tail configuration. In a recent study, KMC was applied to understand the branching topology and MWD during the high-pressure polymerization of ethylene. The complete branching architecture of the polymer chains was then utilized to evaluate the rheological properties of the polymer using random-walk simulations (124).

Another area in which KMC has been useful is in predicting the sequence distribution of gradient copolymers, which exhibit a continuous change in composition or segment length along the copolymer chain. Experimental determination of the explicit monomer sequences is challenging,

as multiple segments along a chain are formed continuously. Wang & Broadbelt (86) have developed a KMC procedure to track the monomer sequences along every individual chain during the NM-CRP of styrene and MMA. The data structure used to track the sequences included mapping the segment length of each type of monomer along the normalized chain location. Although the polymers, poly(styrene-*grad*-MMA) and poly(MMA-*grad*-styrene), exhibited strong compositional gradients, the number average segment lengths were short (2–4), and the sequence length distribution resembled that of random copolymers. One of the primary advantages of KMC is that it can be used as a predictive tool to design reaction conditions according to specified end properties such as M_n, PDI, and copolymer microstructure (125). For example segment lengths greater than four can be obtained only when the monomer feed profile of the type of monomer comprising the given segment is high and the nitroxide concentration is low (87). Such details are valuable inputs to the experimental design of gradient copolymers for high-end applications.

Although the above discussion has illustrated that KMC is a valuable modeling technique and is more attractive than continuum models for polymers, KMC can be much slower and more computationally prohibitive, especially for systems that contain many species and reaction channels (as in pyrolysis and oxidation) owing to the scope of the mechanism. Hence, an optimal trade-off between model complexity and solution methodology is sought.

CURRENT STATUS OF MODELING OF BIOMASS CONVERSION

The generation of fuels and fine chemicals from biomass, a clean, sustainable, and renewable energy source, is one of the top priorities of the twenty-first century. Lignocellulosic biomass, which refers to plant and plant-derived matter produced by photosynthesis, is chemically composed of cellulose, hemicellulose, and lignin. The three main strategies to convert biomass to liquid fuels and refinery intermediates are gasification, fast pyrolysis/liquefaction, and (enzymatic and catalytic) hydrolysis. For more detailed scientific and engineering aspects of the above processes, the interested reader is referred to reviews by Huber et al. (126), Mohan et al. (127), and Serrano-Ruiz et al. (128). Although an understanding of the mechanism and kinetics of all three processes above is crucial to further development, we here focus on the challenges and opportunities in modeling biomass fast pyrolysis, which is a promising and cost-effective technique to produce bio-crude/bio-oil.

Challenges in Modeling Biomass Fast Pyrolysis

Fast pyrolysis of biomass generates 60–75 wt% of liquid bio-oil, 15–25 wt% of solid char, and 10–20 wt% of noncondensable gases (127). Bio-oil, a complex mixture of oxygenated organic compounds, can be upgraded to fuels or refinery intermediates. It is, hence, imperative that process models predict the bio-oil composition before it is sent to a catalytic upgrading or deoxygenation stage. Currently, the successful modeling of fast pyrolysis reactors is hampered by lumped kinetic models, which fail to predict the bio-oil composition. These kinetic models lump similar species according to their molecular weight and are usually stoichiometric or yield based, i.e., the yields of the various fractions are specified rather than predicted. The well-known Broido-Shafizadeh scheme involves the following limited steps for the transformation of cellulose (C) through activated cellulose (C*) to various products: $C \xrightarrow{k_1} C^* \xrightarrow{k_2}$ volatile species, and $C^* \xrightarrow{k_3} 0.35$ char + 0.65 gases (129). Many variants of such global schemes are available in the literature (130, 131). The rate coefficients in these models are usually determined by fitting experimental thermogravimetric data and are, hence, mechanism free. Thus, the rate coefficients for these lumped schemes span a wide range, as they depend significantly on feedstock composition and reaction conditions.

Moreover, the material that has been claimed to be activated cellulose or activated biomass is yet to be structurally validated, although many studies propose that it is a partly cross-linked structure owing to the rupture of intermolecular H-bonds (132). All these substantiate the need for an improved fundamental understanding of the pathways that lead to the various products in bio-oil. However, there are significant challenges in developing a detailed mechanistic model of biomass fast pyrolysis.

1. First, the molecular structure of biomass is not fully understood. Although cellulose has a regular structure of repeating glucose units, hemicellulose contains a mixture of glucose, galactose, mannose, xylose, arabinose, and glucuronic acid units in the chain, which is also branched. Lignin is composed of coniferyl, sinapyl, and *p*-coumaryl alcohol as the basic building units, but as these building blocks are highly cross-linked, only proposed structures of lignin are currently available. Hence, a realistic assumption of the structure of biomass is the first step in developing mechanistic models.
2. The products of fast pyrolysis are often distributed in all three phases, with frequent interconversion between phases. For example, the primary liquids/aerosols that are produced by the rapid heating of biomass ($>1{,}000°C\ s^{-1}$) condense to bio-oil, which on longer exposure to high temperature condenses to char or noncondensable gases. Hence, it is crucial to differentiate the primary and secondary reactions of fast pyrolysis and to understand at what conditions such transformations happen.
3. The product yields are strictly dependent on temperature, pressure, residence time, biomass composition, and the presence of mineral matter (such as inorganic salts and metal ions) in biomass. Even ppm levels of inorganic salts drastically affect the yields of the major products of cellulose fast pyrolysis (133). For example, the yield of levoglucosan drops from 59 wt% to approximately 15 wt%, with a concomitant increase in char and C1–C4 LMWP yields, when 0.30–0.40 mmol of alkali or alkaline earth metal chlorides are added per gram of cellulose. This suggests that metal cations and anions may selectively bind to glycosidic oxygen and prevent the glycosidic bond cleavage, which is the first step in the formation of levoglucosan. Alternatively, the metal ions might also act by reducing the energy barrier of dehydration reactions, thereby promoting the yield of other LMWPs. Hence, it is important to understand whether mineral matter alters the energy barrier of a particular reaction or changes the entire reaction pathway.
4. Although it is well established that synthetic polymers degrade during pyrolysis by a free radical mechanism, biomass fast pyrolysis involves a mix of free radical chemistry, ionic chemistry, and concerted pathways for the formation of products. Therefore, it is essential to identify the mechanism followed by each individual component of biomass to create a kinetic scheme. Mechanistic studies of the pyrolysis of model compounds play an important role in unraveling the reaction pathways of the individual components, which can be later integrated to represent the entire biomass (134).

Current Status and Future Issues

Phenethyl phenyl ether (PPE) is one of the well-studied model lignin compounds owing to its β-ether linkage, which characterizes more than 50% of the interunit linkages in lignin. Klein & Virk (134, 135), and Britt and coworkers (136–138) studied the thermal decomposition of PPE to unravel the reaction mechanism. Britt et al. (136) investigated the selectivity of two pathways, namely, reactions of the α- and β-radical of PPE, for the formation of styrene and phenol as the major primary products and toluene and benzaldehyde as the minor products, respectively. The α/β selectivity of 3.1 ± 0.3 was invariant with temperature and PPE concentration in both

the liquid and the gas phase, whereas the presence of H-donor solvents drastically increased the selectivity. **Supplemental Figure 3** depicts the key reactions involved in the transformation of PPE according to a kinetic analysis of the reactions by quantum chemical calculations (138). In a recent study, Jarvis et al. (139) utilized a hyperthermal nozzle coupled with mass spectrometry as well as ab initio quantum chemical calculations to identify the various free radicals and evaluate the kinetic parameters during the pyrolysis of PPE. At moderate temperatures corresponding to fast pyrolysis, concerted pathways such as the 6-centered retro-ene reaction and the 4-centered Maccoll elimination dominate the pathways for the formation of styrene and phenol, whereas the free radical pathways dominate at temperatures greater than 1,000°C, which correspond to gasification.

The barriers to the development of mechanistic models of biomass fast pyrolysis are twofold. First, the kinetics of many elementary steps for the formation of products still remain unexplored, and second, time evolution data for the individual pyrolysis products are yet to be experimentally obtained owing to the short reaction time (~1 s). One of the important transformations that requires attention is the formation of levoglucosan from cellulose. Although it is speculated that levoglucosan is formed via homolytic, heterolytic, and concerted pathways, there is no definitive pathway in terms of the kinetics of the transformation. The various possible pathways are depicted in **Supplemental Figure 4**. In this regard, synergistic efforts between the experimental and modeling communities are vital. Highly detailed ^{13}C-NMR labeling studies would aid in the identification of important pathways, which can be investigated in more detail by using quantum chemistry to unravel the kinetics. For example, Paine III et al. (140) have used isotopic ^{13}C labeling studies to identify the various reactions in glucose pyrolysis leading to the formation of C1–C4 carbonyl compounds and furans by electrocyclic fragmentation mechanisms. Recently, many DFT and ab initio studies have investigated the kinetics of elementary reactions such as dehydration, retro-aldol, retro-Diels-Alder, ring opening, ring flipping, and Grob fragmentation in glucose and cellulose pyrolysis (141–143). Moreover, detailed studies of fast pyrolysis of pure and mineral-impregnated cellulose, hemicellulose, and lignin with quantitative speciation data would help in formulating a baseline model of noncatalytic fast pyrolysis (144–146) that can be extended in real time to catalytic fast pyrolysis by computationally studying the energetics of only the relevant reactions over the catalysts.

Furthermore, in the model development process, lumping of species clearly is necessary to handle the structural complexity involved in various species and the computational cost. The only semidetailed model available today is that of lignin pyrolysis proposed by Faravelli et al. (8); its lumping scheme includes the important linkages and substructures in lignin. The model, consisting of 100 molecular and radical species in 500 elementary and lumped reactions, satisfactorily captured the devolatilization profiles of slow pyrolysis of a range of lignins from different sources. Recently, reaction-generation tools specific to reaction chemistries that occur in biomass conversion have also been developed. The computational platform, dubbed the Rule Input Network Generator, reproduced all the reactions reported in the literature for the homogeneous and heterogeneous thermochemical conversion reactions of small biomass model compounds (147). Although the current developments in modeling biomass conversion are promising, substantial work remains to achieve a mechanistic model.

SUMMARY

Mechanistic kinetic models seek to describe chemical reactions at a molecular level, and the wealth of information that is obtained from a mechanistic model can even surpass what is available from experiments. Undoubtedly, mechanistic models are central to chemical engineering process

design, development, and optimization. In this review of the modeling process, we have examined the fundamental elements of mechanistic models as applied to complex polymeric systems. The elementary steps in the free radical chain reaction mechanism of pyrolysis and oxidation are well understood and serve as the foundation of the kinetic models. Assigning accurate values of the rate coefficients of the elementary steps is the heart of a successful kinetic model, and this can be achieved through GA-based estimates, quantum chemistry calculations, or structure-activity relationships to supplement experimental values, which are not available for most of the reactions. Additionally, polymeric systems warrant the inclusion of the chain-length dependency of the termination rate coefficient to describe the kinetics. Lumping the polymer chains on the basis of the structure of the end groups greatly aids in tracking the course of the reaction and unraveling reaction pathways. Although both moment-based and KMC approaches are valuable in synthesizing the intricate details of the polymer during reaction, the solution methodology needs to be selected by assessing the scope of the mechanism, the detail desired, and the computational resources.

DISCLOSURE STATEMENT

The authors are not aware of any affiliations, memberships, funding, or financial holdings that might be perceived as affecting the objectivity of this review.

ACKNOWLEDGMENTS

The authors are grateful for financial support by the MRSEC program of the National Science Foundation (DMR-0520513) at the Materials Research Center of Northwestern University and the Department of Energy (DOE) Office of Energy Efficiency and Renewable Energy (EERE) through the Office of Biomass Program, grant number DE-EE0003044.

LITERATURE CITED

1. Khan SS, Zhang Q, Broadbelt LJ. 2009. Automated mechanism generation. Part 1: Mechanism development and rate constant estimation for VOC chemistry in the atmosphere. *J. Atmos. Chem.* 63:125–56
2. Khan SS, Broadbelt LJ. 2009. Automated mechanism generation. Part 2: Application to atmospheric chemistry of alkanes and oxygenates. *J. Atmos. Chem.* 63:157–86
3. Rabek JF. 1996. *Photodegradation of Polymers: Physical Characteristics and Applications*. Berlin: Springer
4. **Ranzi E, Dente M, Goldaniga A, Bozzano G, Faravelli T. 2001. Lumping procedures in detailed kinetic modeling of gasification, pyrolysis, partial oxidation and combustion of hydrocarbon mixtures. *Prog. Energy Combust. Sci.* 27:99–139**
5. **Kruse TM, Woo OS, Wong H-W, Khan SS, Broadbelt LJ. 2002. Mechanistic modeling of polymer degradation: a comprehensive study of polystyrene. *Macromolecules* 35:7830–44**
6. Wong H-W, Li X, Swihart MT, Broadbelt LJ. 2004. Detailed kinetic modeling of silicon nanoparticle formation chemistry via automated mechanism generation. *J. Phys. Chem. A* 108:10122–32
7. West RH, Celnik MS, Inderwildi OR, Kraft M, Beran GJO, Green WH. 2007. Toward a comprehensive model of the synthesis of TiO_2 particles from $TiCl_4$. *Ind. Eng. Chem. Res.* 46:6147–56
8. Faravelli T, Frassoldati A, Migliavacca G, Ranzi E. 2010. Detailed kinetic modeling of the thermal degradation of lignins. *Biomass Bioenergy* 34:290–301
9. Rice FO. 1935. The decomposition of organic compounds from the standpoint of free radicals. *Chem. Rev.* 17:53–63
10. Clymans PJ, Froment GF. 1984. Computer-generation of reaction paths and rate equations in the thermal cracking of normal and branched paraffins. *Comput. Chem. Eng.* 8:137–42
11. Hillewaert LP, Dierickx JL, Froment GF. 1988. Computer generation of reaction schemes and rate equations for thermal cracking. *AIChE J.* 34:17–24

4. Illustrates the use of lumping and simplifying rules to construct a mechanistic model for complex hydrocarbon chemistries.

5. Details the various steps involved in developing a mechanistic model for polymer pyrolysis.

12. Quann RJ, Jaffe SB. 1992. Structure-oriented lumping: describing the chemistry of complex hydrocarbon molecules. *Ind. Eng. Chem. Res.* 31:2483–97
13. Broadbelt LJ, Stark SM, Klein MT. 1994. Computer generated pyrolysis modeling: on-the-fly generation of species, reaction, and rates. *Ind. Eng. Chem. Res.* 33:790–99
14. Chevalier C, Warnatz J, Melenk J. 1990. Automatic generation of reaction mechanisms for description of oxidation of higher hydrocarbons. *Ber. Bunsen-Ges. Phys. Chem.* 94:1362–67
15. Susnow RG, Dean AM, Green WH, Peczak P, Broadbelt LJ. 1997. Rate-based construction of kinetic models for complex systems. *J. Phys. Chem. A* 101:3731–40
16. Mitsos A, Oxberry GM, Barton PI, Green WH. 2008. Optimal automatic reaction and species elimination in kinetic mechanisms. *Combust. Flame* 155:118–32
17. Wei W, Bennett CA, Tanaka R, Hou G, Klein MT Jr, Klein MT. 2008. Computer aided kinetic modeling with KMT and KME. *Fuel Process. Technol.* 89:350–63
18. Kee RJ, Rupley FM, Miller JA, Coltrin ME, Grcar JF, et al. 2000. *Chemkin Collection*, release 3.6. Reaction Design Inc., San Diego, CA.
19. Detailed Chemistry in CFD. **http://www.detchem.com/**
20. Naik CV, Dean AM. 2006. Detailed kinetic modeling of ethane oxidation. *Combust. Flame* 145:16–37
21. Curran HJ, Gaffuri P, Pitz WJ, Westbrook CK. 2002. A comprehensive modeling study of *n*-heptane oxidation. *Combust. Flame* 114:149–77
22. Curran HJ, Gaffuri P, Pitz WJ, Westbrook CK. 2002. A comprehensive modeling study of iso-octane oxidation. *Combust. Flame* 129:253–80
23. Dagaut P, Hadj-Ali K. 2009. Chemical kinetic study of the oxidation of isocetane (2,2,4,4,6,8,8-heptamethylnonane) in a jet-stirred reactor: experimental and modeling. *Energy Fuels* 23:2389–95
24. Oehlschlaeger MA, Shen H-PS, Frassoldati A, Pierucci S, Ranzi E. 2009. Experimental and kinetic modeling study of the pyrolysis and oxidation of decalin. *Energy Fuels* 23:1464–72
25. Matheu DM, Dean AM, Grenda JM, Green WH Jr. 2003. Mechanism generation with integrated pressure dependence: a new model for methane pyrolysis. *J. Phys. Chem. A* 107:8552–65
26. Randolph KL, Dean AM. 2007. Hydrocarbon fuel effects in solid-oxide fuel cell operation: an experimental and modeling study of *n*-hexane pyrolysis. *Phys. Chem. Chem. Phys.* 9:4245–58
27. Klein MT, Hou G, Bertolacini RJ, Broadbelt LJ, Kumar A. 2006. *Molecular Modeling in Heavy Hydrocarbon Conversions*. Boca Raton, FL: CRC Press
28. Poutsma ML. 1990. Free-radical thermolysis and hydrogenolysis of model hydrocarbons relevant to processing of coal. *Energy Fuels* 4:113–31
29. Poutsma ML. 2000. Fundamental reactions of free radicals relevant to pyrolysis reactions. *J. Anal. Appl. Pyrolysis* 54:5–35
30. Savage PE. 2000. Mechanisms and kinetic models for hydrocarbon pyrolysis. *J. Anal. Appl. Pyrolysis* 54:109–26
31. Moad G, Solomon DH. 2006. *The Chemistry of Radical Polymerization*. Oxford, UK: Elsevier. 2nd ed.
32. Faravelli T, Pinciroli M, Pisano F, Bozzano G, Dente M, Ranzi E. 2001. Thermal degradation of polystyrene. *J. Anal. Appl. Pyrolysis* 60:103–21
33. Poutsma ML. 2006. Mechanistic analysis and thermochemical kinetic simulation of the pathways for volatile product formation from pyrolysis of polystyrene, especially for the dimer. *Polym. Degrad. Stab.* 91:2979–3009
34. Levine SE, Broadbelt LJ. 2008. Reaction pathways to dimer in polystyrene pyrolysis: a mechanistic modeling study. *Polym. Degrad. Stab.* 93:941–51
35. Poutsma ML. 2009. Further considerations of the sources of the volatiles from pyrolysis of polystyrene. *Polym. Degrad. Stab.* 94:2055–64
36. Kruse TM, Wong H-W, Broadbelt LJ. 2003. Mechanistic modeling of polymer pyrolysis: polypropylene. *Macromolecules* 36:9594–607
37. Levine SE, Broadbelt LJ. 2009. Deatailed mechanistic modeling of high-density polyethylene pyrolysis: low molecular weight product evolution. *Polym. Degrad. Stab.* 93:810–22
38. Marongiu A, Faravelli T, Ranzi E. 2007. Detailed kinetic modeling of the thermal degradation of vinyl polymers. *J. Anal. Appl. Pyrolysis* 78:343–62

27. Covers the basics of and development of tools for the construction, solution, and optimization of detailed mechanistic models.

39. Poutsma ML. 2003. Reexamination of the pyrolysis of polyethylene: data needs, free-radical mechanistic considerations, and thermochemical kinetic simulation of initial product-forming pathways. *Macromolecules* 36:8931–57
40. Pfaendtner J, Broadbelt LJ. 2008. Mechanistic modeling of lubricant degradation. 2. The autoxidation of decane and octane. *Ind. Eng. Chem. Res.* 47:2897–904
41. Pfaendtner J, Broadbelt LJ. 2008. Mechanistic modeling of lubricant degradation. 1. Structure-reactivity relationships for free-radical oxidation. *Ind. Eng. Chem. Res.* 47:2886–96
42. Ranzi E, Frassoldati A, Granata S, Faravelli T. 2005. Wide-range kinetic modeling study of the pyrolysis, partial oxidation, and combustion of heavy *n*-alkanes. *Ind. Eng. Chem. Res.* 44:5170–83
43. Gryn'ova G, Hodgson JL, Coote ML. 2011. Revising the mechanism of polymer autooxidation. *Org. Biomol. Chem.* 9:480–90
44. Vinu R, Levine SE, Wang L, Broadbelt LJ. 2011. Detailed mechanistic modeling of poly(styrene peroxide) pyrolysis using kinetic Monte Carlo simulation. *Chem. Eng. Sci.* 69:456–71

45. Presents propagation and termination rate coefficients for various polymer systems determined by PLP-SEC.

45. Beuermann S, Buback M. 2002. Rate coefficients of free-radical polymerization deduced from pulsed laser experiments. *Prog. Polym. Sci.* 27:191–254

46. Allara DL, Shaw R. 1980. A compilation of kinetic parameters for the thermal degradation of *n*-alkane molecules. *J. Phys. Chem. Ref. Data* 9:523–59
47. NIST Chemical Kinetics Database. 2011. *Standard Reference Database 17*. Version 7.0, Release 1.6.1. **http://kinetics.nist.gov/kinetics/index.jsp**
48. NDRL/NIST Solution Kinetics Database on the Web. 2002. *NIST Standard Reference Database 40*. **http://kinetics.nist.gov/solution/**
49. Benson SW. 1976. *Thermochemical Kinetics: Methods for the Estimation of Thermochemical Data and Rate Parameters*. New York: John Wiley and Sons. 2nd ed.
50. NIST Chemistry Webbook. 2011. *NIST Standard Reference Database 69*. **http://webbook.nist.gov/chemistry/**
51. Willems PA, Froment GF. 1988. Kinetic modeling of the thermal cracking of hydrocarbons. 1. Calculation of frequency factors. *Ind. Eng. Chem. Res.* 27:1959–66
52. Willems PA, Froment GF. 1988. Kinetic modeling of the thermal cracking of hydrocarbons. 2. Calculation of activation energies. *Ind. Eng. Chem. Res.* 27:1966–71

53. Describes rate constant estimation for various reaction families using a group additivity approach combined with ab initio quantum calculations.

53. Sumathi R, Green WH Jr. 2002. A priori rate constants for kinetic modeling. *Theor. Chem. Acc.* 108:187–213

54. Saeys M, Reyniers M-F, Marin GB, Van Speybroeck V, Waroquier M. 2006. Ab initio group contribution method for activation energies for radical additions. *AIChE J.* 50:426–44
55. Saeys M, Reyniers M-F, Van Speybroeck V, Waroquier M, Marin GB. 2006. Ab initio group contribution method for activation energies of hydrogen abstraction reactions. *ChemPhysChem* 7:188–99
56. Sabbe MK, Reyniers M-F, Van Speybroeck V, Waroquier M, Marin GB. 2008. Carbon-centered radical addition and β-scission reactions: modeling of activation energies and pre-exponential factors. *ChemPhysChem* 9:124–40
57. Sabbe MK, Vandeputte AG, Reyniers M-F, Waroquier M, Marin GB. 2010. Modeling the influence of resonance stabilization on the kinetics of hydrogen abstractions. *Phys. Chem. Chem. Phys.* 12:1278–98

58. Provides a dictionary of quantitative kinetic modeling with an emphasis on computational quantum chemistry calculations.

58. Broadbelt LJ, Pfaendtner J. 2005. Lexicography of kinetic modeling of complex reaction networks. *AIChE J.* 51:2112–21

59. Coote ML. 2009. Quantum-chemical modeling of free-radical polymerization. *Macromol. Theory Simul.* 18:388–400
60. Izgorodina EI, Coote ML. 2006. Accurate ab initio prediction of propagation rate coefficients in free-radical polymerization: acrylonitrile and vinyl chloride. *Chem. Phys.* 324:96–110
61. Van Cauter K, Van Speybroeck V, Vansteenkiste P, Reyniers M-F, Waroquier M. 2006. Ab initio study of free-radical polymerization: polyethylene propagation kinetics. *ChemPhysChem* 7:131–40
62. Bebe S, Yu X, Hutchinson RA, Broadbelt LJ. 2006. Estimation of free radical polymerization rate coefficients using computational chemistry. *Macromol. Symp.* 243:179–89
63. Yu X, Levine SE, Broadbelt LJ. 2008. Kinetic study of the copolymerization of methyl methacrylate and methyl acrylate using quantum chemistry. *Macromolecules* 41:8242–51

64. Dossi M, Liang K, Hutchinson RA, Moscatelli D. 2010. Investigation of free-radical copolymerization propagation kinetics of vinyl acetate and methyl methacrylate. *J. Phys. Chem. B* 114:4213–22
65. Van Cauter K, Van Speybroeck V, Waroquier M. 2007. Ab initio study of poly(vinyl chloride) propagation kinetics: head-to-head versus head-to-tail additions. *ChemPhysChem* 8:541–52
66. Evans MG, Polanyi M. 1938. Inertia and driving force of chemical reactions. *Trans. Farad. Soc.* 34:11–29
67. Fleischer G, Appel M. 1995. Chain length dependence of the self-diffusion of polyisoprene and polybutadiene in the melt. *Macromolecules* 28:7281–83
68. Schreck VA, Serelis AK, Solomon DH. 1989. Self-reactions of 1,3-diphenylpropyl and 1,3,5-triphenylpentyl radicals: models for termination in styrene polymerization. *Aust. J. Chem.* 42:375–93
69. Konar RS. 1970. The disproportionation and combination of alkyl radicals. *Int. J. Chem. Kinet.* 2:419–22
70. Rossi M, King KD, Golden DM. 1978. The equilibrium constant and rate constant for allyl radical recombination in the gas phase. *J. Am. Chem. Soc.* 101:1223–30
71. Klein R, Kelly RD. 1975. Combination and disproportionation of allylic radicals at low temperatures. *J. Phys. Chem.* 79:1780–84
72. Carstensen H-H, Dean AM. 2009. Rate constant rules for the automated generation of gas-phase reaction mechanisms. *J. Phys. Chem. A* 113:367–80
73. Carstensen H-H, Dean AM. 2010. Development of detailed kinetic models for the thermal conversion of biomass via first principle methods and rate estimation rules. In *Computational Modeling in Lignocellulosic Biofuel Production*, ACS Symp. Series 1052, ed. MR Nimlos, MF Crowley, pp. 201–43. Washington, DC: Am. Chem. Soc.
74. Choo KY, Benson SW. 1981. Arrhenius parameters for the alkoxy radical decomposition reactions. *Int. J. Chem. Kinet.* 13:833–44
75. Pfaendtner J, Broadbelt LJ. 2007. Contra-thermodynamic behavior in intermolecular hydrogen transfer of alkylperoxy radicals. *ChemPhysChem* 8:1969–78
76. Blowers P, Masel RI. 1999. An extension of the Marcus equation for atom transfer reactions. *J. Phys. Chem. A* 103:7047–54
77. Fischer H, Radom L. 2001. Factors controlling the addition of carbon-centered radicals to alkenes—an experimental and theoretical perspective. *Angew. Chem. Int. Ed.* 40:1340–71
78. Nyden MR, Stoliarov SI, Westmoreland PR, Guo ZX, Jee C. 2004. Applications of reactive molecular dynamics to the study of the thermal decomposition of polymers and nanoscale structures. *Mater. Sci. Eng. A* 365:114–21
79. Strachan A, Kober EM, van Duin ACT, Oxgaard J, Goddard WA III. 2005. Thermal decomposition of RDX from reactive molecular dynamics. *J. Chem. Phys.* 122:054502
80. Stoliarov SI, Westmoreland PR, Nyden MR, Forney GP. 2003. A reactive molecular dynamics model of thermal decomposition in polymers: I. Poly(methyl methacrylate). *Polymer* 44:883–94
81. Stoliarov SI, Lyon RE, Nyden MR. 2004. A reactive molecular dynamics model of thermal decomposition in polymers: II. Polyisobutylene. *Polymer* 45:8613–21
82. Rouse PE Jr. 1953. A theory of the linear viscoelastic properties of dilute solutions of coiling polymers. *J. Chem. Phys.* 21:1271–80
83. de Gennes PG. 1982. Kinetics of diffusion-controlled processes in dense polymer systems. II. Effects of entanglements. *J. Chem. Phys.* 76:3322–26
84. Keramopoulos A, Kiparissides C. 2002. Development of a comprehensive model for diffusion-controlled free-radical copolymerization reaction. *Macromolecules* 35:4155–66
85. Ismail H, Abel PR, Green WH, Fahr A, Jusinski LE, et al. 2009. Temperature-dependent kinetics of the vinyl radical (C_2H_3) self-reaction. *J. Phys. Chem. A* 113:1278–86
86. Wang L, Broadbelt LJ. 2009. Explicit sequence of styrene/methyl methacrylate gradient copolymers synthesized by forced gradient copolymerization with nitroxide-mediated controlled radical polymerization. *Macromolecules* 42:7961–68
87. Wang L, Broadbelt LJ. 2009. Factors affecting the formation of the monomer sequence along styrene/methyl methacrylate gradient copolymer chains. *Macromolecules* 42:8118–28
88. Kodera Y, McCoy BJ. 1997. Distribution kinetics of radical mechanisms: reversible polymer decomposition. *AIChE J.* 43:3205–14

89. Wang M, Smith JM, McCoy BJ. 1995. Continuous kinetics for thermal degradation of polymer in solution. *AIChE J.* 41:1521–33
90. Sterling WJ, McCoy BJ. 2001. Distribution kinetics of thermolytic macromolecular reactions. *AIChE J.* 47:2289–303
91. Kruse TM, Levine SE, Wong H-W, Duoss E, Lebovitz AH, et al. 2005. Binary mixture pyrolysis of polypropylene and polystyrene: a modeling and experimental study. *J. Anal. Appl. Pyrolysis* 73:342–54
92. Kruse TM, Woo OS, Broadbelt LJ. 2001. Detailed mechanistic modeling of polymer degradation: application to polystyrene. *Chem. Eng. Sci.* 56:971–79
93. Marongiu A, Faravelli T, Bozzano G, Dente M, Ranzi E. 2003. Thermal degradation of poly(vinyl chloride). *J. Anal. Appl. Pyrolysis* 70:519–53
94. McCoy BJ, Madras G. 1998. Evolution to similarity solutions for fragmentation and aggregation. *J. Colloid Interf. Sci.* 201:200–9
95. Madras G, McCoy BJ. 2002. Numerical and similarity solutions for reversible population balance equations with size-dependent rates. *J. Colloid Interf. Sci.* 246:356–65
96. Ziff RM, McGrady ED. 1986. Kinetics of polymer degradation. *Macromolecules* 19:2513–19
97. Family F, Meakin P, Deutch JM. 1986. Kinetics of coagulation with fragmentation: scaling behavior and fluctuations. *Phys. Rev. Lett.* 57:727–30
98. Vigil RD, Ziff RM. 1989. On the stability of coagulation-fragmentation population balances. *J. Colloid Interface Sci.* 133:257–64
99. Saidel GM, Katz S. 1968. Dynamic analysis of branching in radical polymerization. *J. Polym. Sci. Part A-2* 6:1149–60
100. Papavasiliou G, Birol İ, Teymour F. 2002. Calculation of molecular weight distributions in non-linear free-radical polymerization using the numerical fractionation technique. *Macromol. Theory Simul.* 11:533–48
101. Vinu R, Madras G. 2009. Continuous distribution kinetics for photopolymerization of alkyl methacrylates. *Macromol. React. Eng.* 3:556–67
102. Pladis P, Kiparissides C. 1998. A comprehensive model for the calculation of molecular weight-long-chain branching distribution in free-radical polymerizations. *Chem. Eng. Sci.* 53:3315–33
103. Gavalas GR. 1966. The long chain approximation in free radical reaction systems. *Chem. Eng. Sci.* 21:133–41
104. Nigam A, Fake DM, Klein MT. 1994. Approximate rate law for both short- and long-chain Rice Herzfeld kinetics. *AIChE J.* 40:908–10
105. Krallis A, Pladis P, Kiparissides C. 2007. Prediction of the bivariate molecular weight-long chain branching distribution in high-pressure low-density polyethylene autoclaves. *Macromol. Theory Simul.* 16:593–609
106. Asteasuain M, Soares M, Lenzi MK, Cunningham M, Sarmoria C, et al. 2007. "Living" free radical polymerization in tubular reactors. I. Modeling of the complete molecular weight distribution using probability generating functions. *Macromol. React. Eng.* 1:622–34
107. Kruse TM, Wong H-W, Broadbelt LJ. 2003. Modeling the evolution of the full polystyrene molecular weight distribution during polystyrene pyrolysis. *Ind. Eng. Chem. Res.* 42:2722–35
108. Cozewith C, Teymour F. 1998. Polymer cross-linking in post-gel region for continuous and batch reactors. *AIChE J.* 44:722–32
109. Kizilel S, Papavasiliou G, Gossage J, Teymour F. 2007. Mathematical model for vinyl-divinyl polymerization. *Macromol. React. Eng.* 1:587–603
110. Dente M, Ranzi E, Goossens AG. 1979. Detailed prediction of olefin yields from hydrocarbon pyrolysis through a fundamental simulation model (SPYRO). *Comput. Chem. Eng.* 3:61–75
111. Stewart WE, Caracotsios M, Sorenson JP. 1994. *Appendix A. DDASAC Software package documentation.* Dept. Chem. Eng., Univ. Wisc., Madison
112. Radhakrishnan K, Hindmarsh AC. 1993. Description and use of LSODE, the Livermore solver for ordinary differential equations. *LLNL Rep. UCRL-ID-113855*, Lawrence Livermore Natl. Lab., Livermore, CA
113. Stewart WE, Caracotsios M, Sorenson JP. 1992. *GREG software package documentation*. Dept. Chem. Eng., Univ. Wisc., Madison

114. Wulkow M. 2008. Computer aided modeling of polymer reaction engineering—the status of Predici, 1: simulation. *Macromol. React. Eng.* 2:461–94
115. Moscatelli D, Cavallotti C, Morbidelli M. 2006. Prediction of molecular weight distributions based on ab initio calculations: application to the high temperature styrene polymerization. *Macromolecules* 39:9641–53
116. Gillespie DT. 1977. Exact stochastic simulation of coupled chemical reactions. *J. Phys. Chem.* 81:2340–61
117. Gillespie DT. 2007. Stochastic simulation of chemical kinetics. *Annu. Rev. Phys. Chem.* 58:35–55
118. Tobita H. 1996. Random degradation of branched polymers. 1. Star polymers. *Macromolecules* 29:3000–9
119. Tobita H. 1996. Random degradation of branched polymers. 2. Multiple branches. *Macromolecules* 29:3010–21
120. Tobita H. 2001. Simultaneous long-chain branching and random scission: I. Monte Carlo simulation. *J. Polym. Sci. Part B* 39:391–403
121. Bose SM, Git T. 2004. Mathematical modeling and computer simulation of linear polymer degradation: simple scissions. *Macromol. Theory Simul.* 13:453–73
122. McDermott JB, Libanati C, LaMarca C, Klein MT. 1990. Quantitative use of model compound information: Monte Carlo simulation of the reactions of complex macromolecules. *Ind. Eng. Chem. Res.* 29:22–29
123. Pinto J-HQ, Kaliaguine S. 1991. A Monte Carlo analysis of acid hydrolysis of glycosidic bonds in polysaccharides. *AIChE J.* 37:905–14
124. Meimaroglou D, Kiparissides C. 2010. A novel stochastic approach for the prediction of the exact topological characteristics and rheological properties of highly-branched polymer chains. *Macromolecules* 43:5820–32
125. Wang L, Broadbelt LJ. 2011. Model-based design for preparing styrene/methyl methacrylate structural gradient copolymers. *Macromol. Theory Simul.* 20:191–204
126. Huber GW, Iborra S, Corma A. 2006. Synthesis of transportation fuels from biomass: chemistry, catalysis and engineering. *Chem. Rev.* 106:4044–98
127. Mohan D, Pittman CU Jr, Steele PH. 2006. Pyrolysis of wood/biomass for bio-oil: a critical review. *Energy Fuels* 20:848–89
128. Serrano-Ruiz JC, West RM, Dumesic JA. 2010. Catalytic conversion of renewable biomass resources to fuels and chemicals. *Annu. Rev. Chem. Biomol. Eng.* 1:79–100
129. Antal MJ Jr, Varhegyi G. 1995. Cellulose pyrolysis kinetics: the current state of knowledge. *Ind. Eng. Chem. Res.* 34:703–17
130. Ranzi E, Cuoci A, Faravelli T, Frassoldati A, Migliavacca G, et al. 2008. Chemical kinetics of biomass pyrolysis. *Energy Fuels* 22:4292–300
131. Di Blasi C. 2008. Modeling chemical and physical processes of wood and biomass pyrolysis. *Prog. Energy Combust. Sci.* 34:47–90
132. Chaiwat W, Hasegawa I, Tani T, Sunagawa K, Mae K. 2009. Analysis of cross-linking behavior during pyrolysis of cellulose for elucidating reaction pathway. *Energy Fuels* 23:5765–72
133. Patwardhan PR, Satrio JA, Brown RC, Shanks BH. 2010. Influence of inorganic salts on the primary pyrolysis products of cellulose. *Biores. Technol.* 101:4646–55
134. Klein MT, Virk PS. 2008. Modeling of lignin thermolysis. *Energy Fuels* 22:2175–82
135. Klein MT, Virk PS. 1983. Model pathways in lignin thermolysis. 1. Phenethyl phenyl ether. *Ind. Eng. Chem. Fundam.* 22:35–45
136. Britt PF, Buchanan AC 3rd, Malcolm EA. 1995. Thermolysis of phenethyl phenyl ether: a model for ether linkages in lignin and low rank coal. *J. Org. Chem.* 60:6523–36
137. Britt PF, Kidder MK, Buchanan AC 3rd. 2007. Oxygen substituent effects in the pyrolysis of phenethyl phenyl ethers. *Energy Fuels* 21:3102–8
138. Beste A, Buchanan AC 3rd, Britt PF, Hathorn BC, Harrison RJ. 2007. Kinetic analysis of the pyrolysis of phenethyl phenyl ether: computational prediction of α/β selectivities. *J. Phys. Chem. A* 111:12118–26
139. Jarvis MW, Daily JW, Carstensen H-H, Dean AM, Sharma S, et al. 2011. Direct detection of products from the pyrolysis of 2-phenethyl phenyl ether. *J. Phys. Chem. A* 115:428–38

117. Excellent review of the different kinetic Monte Carlo simulation techniques.

125. Describes the development of a design tool to generate recipes for structural gradient copolymers.

134. Provides a modeling framework to synthesize the thermolysis data of lignin model compounds to describe the behavior of actual lignin.

140. Paine JB III, Pithawalla YB, Naworal JD. 2008. Carbohydrate pyrolysis mechanisms from isotopic labeling. Part 4. The pyrolysis of D-glucose: the formation of furans. *J. Anal. Appl. Pyrolysis* 83:37–63
141. Nimlos MR, Blanksby SJ, Ellison GB, Evans RJ. 2003. Enhancement of 1,2-dehydration of alcohols by alkali cations and protons: a model for dehydration of carbohydrates. *J. Anal. Appl. Pyrolysis* 66:3–27
142. Huang J, Liu C, Wei S, Huang X, Li H. 2010. Density functional theory studies on pyrolysis mechanism of β-D-glucopyranose. *J. Mol. Struct.: THEOCHEM* 958:64–70
143. Zhang M, Geng Z, Yu Y. 2011. Density functional theory (DFT) study on the dehydration of cellulose. *Energy Fuels* 25:2664–70
144. Lin Y-C, Cho J, Tompsett GA, Westmoreland PR, Huber GW. 2009. Kinetics and mechanism of cellulose pyrolysis. *J. Phys. Chem. C* 113:20097–107
145. Patwardhan PR, Brown RC, Shanks BH. 2011. Product distribution from the fast pyrolysis of hemicellulose. *ChemSusChem* 4:636–43
146. Patwardhan PR, Satrio JA, Brown RC, Shanks BH. 2009. Product distribution from fast pyrolysis of glucose-based carbohydrates. *J. Anal. Appl. Pyrolysis* 86:323–30
147. Rangarajan S, Bhan A, Daoutidis P. 2010. Rule-based generation of thermochemical routes to biomass conversion. *Ind. Eng. Chem. Res.* 49:10459–70

146. Provides detailed speciation data for the various constituents in bio-oil from fast pyrolysis of glucose-based carbohydrates.

Annual Review of Chemical and Biomolecular Engineering

Volume 3, 2012

Contents

Indexes

Errata

An online log of corrections to *Annual Review of Chemical and Biomolecular Engineering* articles may be found at http://chembioeng.annualreviews.org/errata.shtml